AIAA 81-4061

# Reduced Basis Technique for Collapse Analysis of Shells

Ahmed K. Noor*
*George Washington University Center at NASA Langley Research Center, Hampton, Va.*
C. M. Andersen†
*College of William and Mary in Virginia, Williamsburg, Va.*
and
Jeanne M. Peters‡
*George Washington University Center at NASA Langley Research Center, Hampton, Va.*

**A hybrid finite-element Rayleigh-Ritz technique is used to predict the collapse behavior of shells. In this hybrid technique, the modeling versatility of the finite-element method is preserved, and a significant reduction in the number of degrees of freedom is achieved by expressing the nodal displacement vector as a linear combination of a small number of basis vectors. A Rayleigh-Ritz technique is used to approximate the finite-element equations of the discretized shell by a reduced system of nonlinear algebraic equations. A scalar function is introduced to measure the degree of nonlinearity of the structure for the case of loading applied by means of axial end shortening. Also, a quantitative measure for the error of the reduced system of equations is proposed. Some insight is given as to why and when the reduced basis technique works, and the effectiveness of the technique for predicting the collapse behavior of shells is demonstrated by means of a numerical example of elastic collapse of an axially compressed pear-shaped cylinder.**

## Nomenclature

| | |
|---|---|
| $E$ | = elastic modulus of the shell material |
| $e$ | = error norm defined in Eq. (16) |
| $\{\mathfrak{F}\}, \{\mathfrak{F}_s\}$ | = vectors of constraint forces defined in Eqs. (1) and (4) |
| $\{\tilde{\mathfrak{F}}\}$ | = vector of constraint forces of the reduced system defined in Eq. (7) |
| $\{G(X)\}$ | = vector of nonlinear terms defined in Eq. (1) |
| $\{G_1\}, \{G_2\}$ | = partitions of the vector $\{G\}$ defined in Eq. (4) |
| $\{\tilde{G}(\psi)\}$ | = vector of nonlinear terms of the reduced equations defined in Eq. (9) |
| $h$ | = thickness of the shell |
| $[K]$ | = global linear stiffness matrix of the shell |
| $[K_{ff}]$, $[K_{fs}]$, $[K_{sf}]$, $[K_{ss}]$ | = partitions of the matrix $[K]$ defined in Eq. (4) |
| $[\tilde{K}]$ | = linear stiffness matrix of the reduced system |
| $n$ | = total number of displacement degrees of freedom |
| $p$ | = total axial load on the shell |
| $R$ | = radius of curvature of the shell |
| $\{R_f\}$ | = residual vector defined in Eq. (15) |
| $r$ | = number of reduced basis vectors |
| $S_{(i)}$ | = current stiffness parameter corresponding to point $i$ of the solution path |
| $U$ | = total strain energy |
| $u_1, u_2, w$ | = displacement components in the coordinate directions (see Fig. 1) |
| $\{X\}$ | = vector of nodal displacements |
| $\{X_f\}$, $\{X_s\}$ | = vectors of free and prescribed (nonzero) nodal displacements |
| $x_1, x_2, x_3$ | = orthogonal curvilinear coordinates (see Fig. 1) |
| $\{Z\}$ | = vector of displacement parameters defined in Eq. (3) |
| $[\Gamma]$ | = matrix of reduced basis vectors defined in Eq. (6) |
| $\lambda$ | = path parameter chosen to be a displacement parameter in the present study |
| $\nu$ | = Poisson's ratio of the material |
| $\phi_1, \phi_2$ | = rotation components (see Fig. 1) |
| $\{\psi\}$ | = vector of coefficients of the reduced equations |

Received Feb. 8, 1980; revision received Sept. 2, 1980. 

*Professor of Engineering and Applied Science. Associate Fellow AIAA.

†Senior Research Associate.

‡Programmer Analyst.

## Introduction

COLLAPSE analysis of complex shell structures having thousands of degrees of freedom is still not economically feasible on present-day computers. Hence, increasing interest has been shown in the application of a hybrid approach which combines contemporary finite elements and classical Rayleigh-Ritz approximations (see, for example, Refs. 1-8).

In this hybrid technique, the modeling versatility of the finite-element method is preserved, and a significant reduction in the number of degrees of freedom is achieved by expressing the nodal displacement vector as a linear combination of a small number of basis vectors. A Rayleigh-Ritz-type technique is used to approximate the finite-element equations of the discretized shell by a reduced system of nonlinear algebraic equations. As would be expected, the effectiveness of the approach depends, to a great extent, on the proper choice of the reduced basis vectors. Various choices for basis vectors were proposed in the literature.[3-6] In Refs. 6 and 7 it was demonstrated that the use of a nonlinear solution and its various order path derivatives (which are commonly used in the static perturbation technique) as basis vectors can result in highly accurate solutions. However, in all the cited references, the structures were subjected to externally applied loads. The case of loading applied by means of axial end shortening, as would occur in a laboratory compression test, was not considered.

The present study is focused on the application of the reduced basis technique to the elastic collapse analysis of shells subjected to prescribed edge displacements (end shortening). Specifically, the objectives of this paper are to: 1) give some insight as to why and when the reduced basis technique works; 2) outline the modifications in the reduced basis technique of Refs. 6 and 7 which are required in the case of prescribed (nonzero) edge displacements; and 3) demonstrate the effectiveness of the proposed technique by means of a numerical example.

The analytical formulation is based on a form of the geometrically nonlinear shallow shell theory with the effects of transverse shear deformation included. A displacement formulation is used with the fundamental unknowns consisting of the three displacement components and the two rotations at each point of the middle surface of the shell. The numerical solutions were obtained by using 16-node quadrilateral elements with bicubic Lagrangian interpolation functions for each of the displacment and rotation components. The computational algorithm presented herein is a modification and an extension of that presented in Ref. 7.

## Mathematical Formulation

### Governing Finite-Element Equations

A total Lagrangian formulation is used and the shell is discretized by using a displacement finite-element model. The governing finite-element equations, for the case of a loading applied by means of axial end shortening, can be cast in the following compact form:

$$[K]\{X\} + \{G(X)\} - \{\mathfrak{F}\} = 0 \tag{1}$$

where $[K]$ is the $n \times n$ linear global stiffness matrix, $n$ the total number of displacement degrees of freedom, $\{X\}$ the vector of nodal displacements, $\{G(X)\}$ the vector of nonlinear terms which is cubic in $\{X\}$ (see Ref. 7), and $\{\mathfrak{F}\}$ the vector of constraint forces.

It is convenient to partition the vector of nodal displacements as follows:

$$\{X\} = \begin{Bmatrix} X_f \\ X_s \end{Bmatrix} \tag{2}$$

where subscripts $f$ and $s$ refer to free and prescribed (nonzero) displacements, respectively. The constrained zero displacements and their associated equations are not included in Eq. (1). The prescribed (nonzero) displacements are assumed to be proportional to a single parameter $\lambda$, i.e.,

$$\{X_s\} = \lambda\{Z\} \tag{3}$$

As the edge displacements are incremented, the value of the parameter $\lambda$ changes, but the components $\{Z\}$ remain constant.

Equation (1) can be conveniently partitioned into two sets of matrix equations as follows:

$$\begin{bmatrix} K_{ff} & K_{fs} \\ K_{sf} & K_{ss} \end{bmatrix} \begin{Bmatrix} X_f \\ X_s \end{Bmatrix} + \begin{Bmatrix} G_1(X_f, X_s) \\ G_2(X_f, X_s) \end{Bmatrix} - \begin{Bmatrix} 0 \\ \mathfrak{F}_s \end{Bmatrix} = 0 \tag{4}$$

If the displacements $\{X_s\}$ are replaced by their prescribed values [using Eq. (3)] in the first set of Eq. (4), the resulting nonlinear algebraic equations can be solved for $\{X_f\}$. The second set of Eq. (4) can then be used to evaluate the constraint forces $\{\mathfrak{F}_s\}$, associated with the prescribed (nonzero) edge displacement $\{X_s\}$.

### Reduced System of Equations

A Rayleigh-Ritz technique is used to replace Eq. (1) by a reduced system of equations. This step is accomplished by approximating the nonlinear solution $\{X\}$ for a particular value of $\lambda$ by a linear combination of $\{X\}$ corresponding to another value of $\lambda$ and a number of its path derivatives (i.e., derivatives of $\{X\}$ with respect to $\lambda$). The approximation can be expressed as follows:

$$\{X\} = [\Gamma]\{\psi\} \tag{5}$$

where

$$[\Gamma]_{n,r} = \left[ \begin{Bmatrix} 0 \\ Z \end{Bmatrix} \quad \begin{Bmatrix} X_f \\ 0 \end{Bmatrix} \quad \frac{\partial}{\partial\lambda}\begin{Bmatrix} X_f \\ 0 \end{Bmatrix} \cdots \frac{\partial^{r-2}}{\partial\lambda^{r-2}}\begin{Bmatrix} X_f \\ 0 \end{Bmatrix} \right] \tag{6}$$

and $\{\psi\}_{r,1}$ is a vector of coefficients (reduced degrees of freedom) which are obtained by solving the following reduced system of nonlinear algebraic equations:

$$[\tilde{K}]\{\psi\} + \{\tilde{G}(\psi)\} - \{\tilde{\mathfrak{F}}\} = 0 \tag{7}$$

subject to the condition $\psi_1 = \lambda$.

The coefficients of the reduced equations, Eq. (7), are given by:

$$[\tilde{K}] = [\Gamma]^T[K][\Gamma] \tag{8}$$

$$\{\tilde{G}(\psi)\} = [\Gamma]^T\{G(\psi)\} \tag{9}$$

$$\{\tilde{\mathfrak{F}}\} = [\Gamma]^T\{\mathfrak{F}\} \tag{10}$$

where the superscript $T$ denotes transposition and $\{G(\psi)\}$ is obtained from $\{G(X)\}$ by replacing $\{X\}$ by its expression in terms of $\{\psi\}$, Eq. (5). Note that $\{\tilde{\mathfrak{F}}\}$ has only one nonzero component, namely, $\tilde{\mathfrak{F}}_1$.

If $\psi_1$ is replaced by its prescribed value $\lambda$ in the last $r-1$ equations of Eq. (7), the resulting nonlinear equations can be solved for the unknowns $\psi_2, \psi_3, \ldots, \psi_r$. The first equation of Eq. (7) can then be used to evaluate $\tilde{\mathfrak{F}}_1$.

The basis vectors in Eq. (6) are obtained by successive differentiation of the finite-element equations of the discretized shell, Eq. (4), and solving the resulting system of linear algebraic equations. Also, as shown in Ref. 7, the evaluation of all basis vectors requires only one matrix factorization.

The criterion for selecting the number of basis vectors proposed in Ref. 6 was adopted in the present study. The criterion is based on monitoring the condition number of the Gram matrix of the basis vectors, and terminating the generation of these vectors when the condition number exceeds a prescribed value. Also, upper and lower limits for the number of basis vectors were chosen to be 7 and 2, respectively.

The computational procedure outlined in Ref. 7 for the efficient evaluation of the basis vectors, generation of the reduced system of equations, automatic selection of the displacement increments, sensing and controlling the errors of the reduced equations is adopted in the present study. However, the scalar $S$ (current stiffness parameter) used to characterize the nonlinear response (see Ref. 9) and the error norm used in Ref. 6 are not applicable to the case of prescribed edge displacements, and therefore are modified as described subsequently.

### Current Stiffness Parameter

In the case of prescribed edge displacement, the scalar $S$ characterizing the nonlinear response is defined as follows:

$$S_{(i)} = \left\{\frac{\partial \mathfrak{F}_s}{\partial\lambda}\right\}^T_{(i)} \{Z\} \Big/ S_{(0)} \quad \text{for the full system} \tag{11a}$$

$$= \frac{\partial \tilde{\mathfrak{F}}_1}{\partial\lambda}\Big|_{(i)} \Big/ S_{(0)} \quad \text{for the reduced system} \tag{11b}$$

where

$$\left\{\frac{\partial \mathfrak{F}_s}{\partial\lambda}\right\} = \left[[K_{sf}] + \left[\frac{\partial G_{2_i}}{\partial x_{f_j}}\right]\right]\left\{\frac{\partial X_f}{\partial\lambda}\right\} + \left[[K_{ss}] + \left[\frac{\partial G_{2_i}}{\partial X_{s_j}}\right]\right]\{Z\} \tag{12}$$

$$\frac{\partial \tilde{\mathfrak{F}}_I}{\partial \lambda} = \sum_{j=1}^{r} \left[ \tilde{K}_{Ij} + \frac{\partial \tilde{G}_I}{\partial \psi_j} \right] \frac{\partial \psi_j}{\partial \lambda} \tag{13}$$

and

$$S_{(0)} = \left\{ \frac{\partial \mathfrak{F}_s}{\partial \lambda} \right\}_{(0)}^{T} \{Z\} \tag{14}$$

The subscript $(i)$ in Eqs. (11) refers to point $i$ of the solution path and the subscript 0 refers to the point $\lambda = 0$.

The current stiffness parameter $S_{(i)}$ defined in Eqs. (11) is similar to that introduced in Ref. 9 for the case of externally applied loads. The parameter $S_{(i)}$ provides a global measure for the stiffness of the structure at point $i$ of the solution path and is easily computed from the reduced system of equations. The selection of displacement increments and the frequency of error sensing are then related to changes in $S$ (see Ref. 7).

The parameter $S_{(i)}$ has an initial value of 1, increases when the structure stiffens and decreases when the structure softens. For stable equilibrium paths, $S$ is positive; for unstable paths, $S$ is negative; and, at limit or collapse points, $S$ is zero.

### Error Norm

To check the accuracy of the solution obtained by the reduced system of equations, Eq. (7), at any value of the parameter $\lambda$, $\{X\}$ is first generated using Eq. (5) and then the residual vector $\{R_f\}$ is computed using the finite-element equations, Eq. (4), where

$$\{R_f\} = [K_{ff}]\{X_f\} + [K_{fs}]\{X_s\} + \{G_I(X_f, X_s)\} \tag{15}$$

An error measure $e$ is defined as follows:

$$e = \sqrt{\{R_f\}^T\{R_f\} / \{\mathfrak{F}_s\}^T\{\mathfrak{F}_s\}} \tag{16}$$

If the error norm $e$ is less than a prescribed tolerance, the solution is continued; otherwise a corrected (or improved) estimate of $\{X_f\}$ is obtained using the Newton-Raphson technique in conjunction with Eq. (4). Then a new set of basis vectors is generated using the technique outlined in Ref. 7.

## Numerical Studies

To test and evaluate the effectiveness of the proposed reduced basis technique, several nonlinear shell problems are solved by this technique. Comparisons are made with solutions based on the full system of equations of the finite-element model. Typical results are presented herein for the elastic collapse analysis of the simply supported pear-shaped cylinder shown in Fig. 1. The problem is one of three used in Ref. 10 to assess the capability of various programs to analyze shell structures. The structure shown in Fig. 1 is similar to an early design of the space shuttle fuselage. The load is applied to the cylinder by means of a uniform axial end shortening which is increased incrementally until the cylinder collapses.

Due to symmetry, only one quarter of the structure was modeled by a grid of $2 \times 16$ finite elements (see Fig. 1) with bicubic Lagrangian interpolation functions for each of the displacement and rotation components (a total of 1446 nonzero displacement degrees of freedom). Finite-difference solutions to this problem using the STAGS (STructural Analysis of General Shells) computer code are presented in Ref. 10 and finite-element solutions using quadrilateral elements are given in Ref. 11.

Typical results that demonstrate the effectiveness of the reduced basis technique are presented in Figs. 2-6 and are discussed subsequently. The variation of the current stiffness parameter $S$ with loading is shown in Fig. 2. An indication of the accuracy of the normal displacement $w$ at the centers of the flat portions, and the strain energies using the reduced basis technique is given in Figs. 3 and 4. The error norms, at various load levels, of the reduced basis technique with six

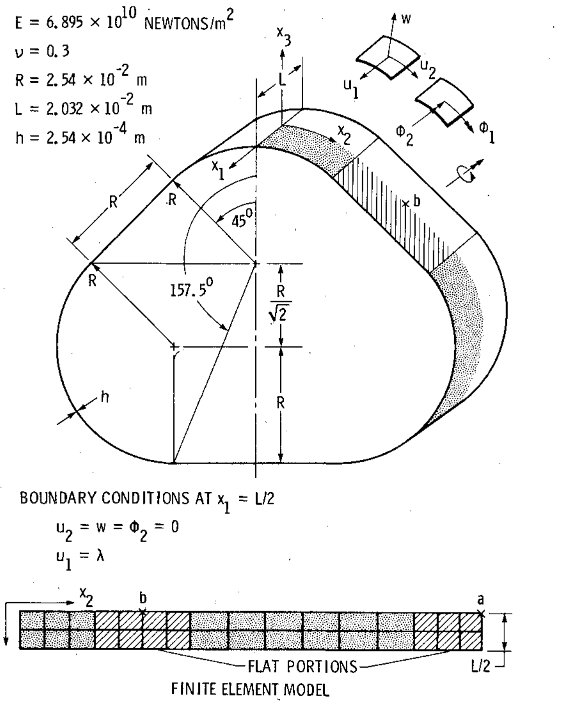


**Fig. 1 Pear-shaped cylinder and finite-element model used in the present study.**

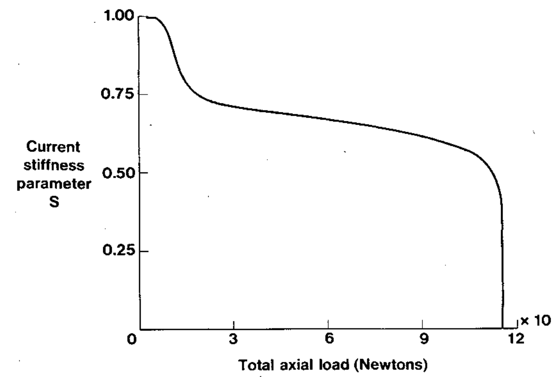


**Fig. 2 Variation of current stiffness parameter with loading for the pear-shaped cylinder shown in Fig. 1.**

and seven basis vectors are shown in Fig. 5. Contour plots of the normal displacement $w$ at different load levels, each normalized by dividing by $w_{max}$ for that load level are shown in Fig. 6.

Three phases can be identified in the solution path (see Fig. 2). The first is a rapid change in stiffness associated with the buckling of the flat portions of the cylinder ($S$ decreases from 1 to 0.75 as $P$ increases from 0 to $1.614 \times 10^3$ N). The second phase is a slow change in stiffness of the structure with an almost linear variation of $S$ with $P$ over the range $P = 1.614 \times 10^3$ to $P = 8.885 \times 10^3$ N. The third phase is that of very rapid change in stiffness of the structure ending with collapse at $P = 11.548 \times 10^3$ N (which is depicted in Fig. 2 by the sharp decrease in $S$, to a negative value, which is not shown in the figure). The collapse loads predicted in Refs. 10 and 11 were $12.455 \times 10^3$ and $10.675 \times 10^3$ N, respectively. Note that the flat portions of the cylinder are in the well-advanced postbuckling stage over a long range of loading (see Figs. 3 and 6).

In the present study the path parameter $\lambda$ was chosen to be equal to the axial end displacements and, therefore, the components for the vector $\{Z\}$ are equal to unity. The basis vectors were first computed for the unloaded shell ($\lambda = 0$, $\{X_f\} = 0$). With a cutoff value of $10^4$ for the condition

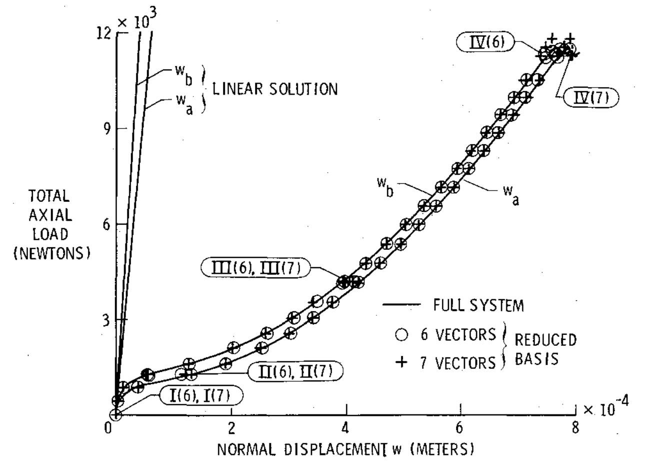


**Fig. 3 Accuracy of normal displacements obtained by reduced basis technique at various load levels. Pear-shaped cylindrical shell shown in Fig. 1. Roman numerals indicate points of generating basis vectors and numbers between parentheses refer to number of basis vectors.**

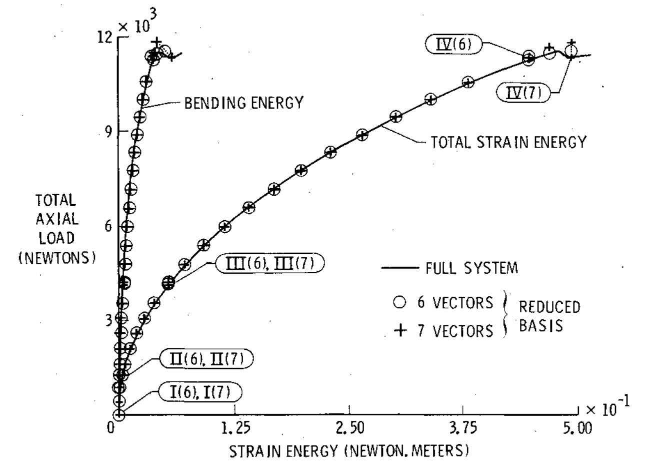


**Fig. 4 Accuracy of strain energies obtained by reduced basis technique at various load levels. Pear-shaped cylindrical shell shown in Fig. 1. Roman numerals indicate points of generating basis vectors and numbers between parentheses refer to number of basis vectors.**

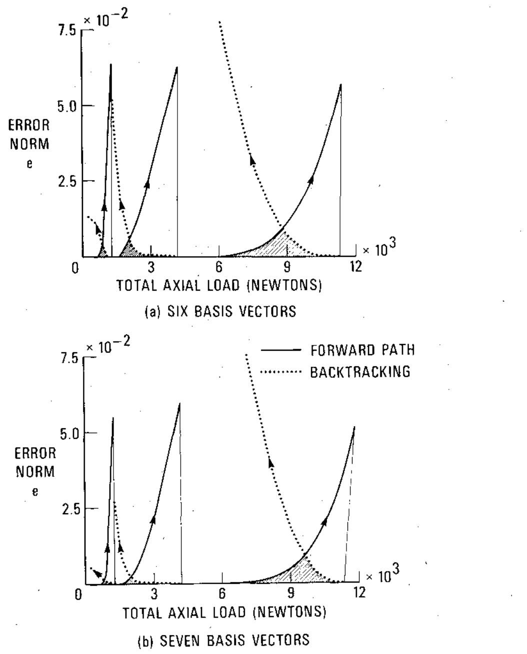


**Fig. 5 Error norms of reduced basis technique at various load levels. Pear-shaped cylindrical shell shown in Fig. 1.**

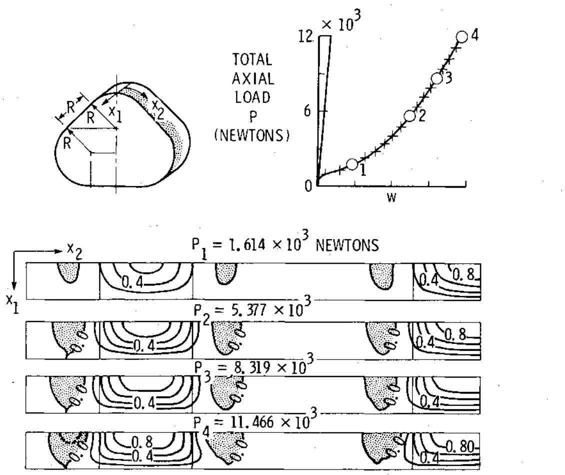


**Fig. 6 Contour plots for the normal displacement $w$ at various load levels (each normalized by dividing by $w_{max}$ for that load level). Pear-shaped cylindrical shell shown in Fig. 1.**

number of the Gram matrix, only six basis vectors were used. When the cutoff value was increased to $10^7$, the number of basis vectors was increased to seven. An error tolerance $e \leq 0.05$ was prescribed. The six and seven basis vectors were each used to advance the solution to $\lambda = 3.048 \times 10^{-6}$ m, at which value the error norms were checked and were found to exceed the prescribed tolerance (see Fig. 5). New (updated) sets of six and seven basis vectors were generated and the solution was continued until $\lambda = 1.219 \times 10^{-5}$ m. The same process was repeated, and new sets of six and seven basis vectors were generated and used to advance the solution until $\lambda = 3.759 \times 10^{-5}$ m for the six vectors and $\lambda = 3.962 \times 10^{-5}$ m for the seven vectors. The latter value of $\lambda$ falls beyond the collapse load of the cylinder (which corresponds to $\lambda = 3.912 \times 10^{-5}$ m).

The high accuracy of the normal displacements and strain energies obtained by the reduced system of equations is demonstrated in Figs. 3 and 4. At $\lambda = 3.759 \times 10^{-5}$ m the errors in the normal displacements $w_a$ and $w_b$ and the total strain energy $U$ obtained by using six basis vectors were 0.55%, 0.36%, and 0.11%, respectively. For seven basis vectors, the corresponding errors at $\lambda = 3.912 \times 10^{-5}$ m were 0.11%, 1.49%, and 0.12%, respectively.

Higher accuracy of the reduced solutions can be achieved by backtracking the equilibrium paths every time a new (updated) basis vector is generated. This amounts to effectively reducing the error norm well below the prescribed tolerance. When this technique was used in the present problem, the maximum values of the error norms using six and seven vectors were reduced to less than 0.016 (see Fig. 5). The computational expense involved in the backtracking process was insignificant.

In summary, the generation of the whole solution path up to collapse of the cylinder involved: 1) generation of an initial set of basis vectors at $\lambda = 0$, and 2) updating the basis vectors three times. The use of the reduced basis technique in this problem resulted in reducing the number of degrees of freedom by a factor of over 200 (from 1446 degrees of freedom for the original finite-element model to six or seven degrees of freedom for the reduced system).

## Comments on the Potential of the Proposed Approach

The following comments concerning why and when the reduced basis technique works seems to be in order:

1) The success of the proposed reduced basis technique can be mainly attributed to the separation of spatial distribution

of the response quantities at any load level from the variation of these quantities with loading. As can be seen from the normalized contour plots of Fig. 6, a large change in loading (or prescribed axial end shortening) is associated with a small change in the spatial distribution of the response quantities (manifested by small changes in the normalized contour plots). Large changes in the normalized contour plots require updating the basis vectors.

2) The particular choice of basis vectors used herein allows highly accurate solutions to be outlined with a small number of basis vectors. Therefore, the time required to solve the reduced system of equations is fairly small and the analysis time, to a first approximation, equals the time required to generate and update the basis vectors.

3) As demonstrated in the numerical example, the efficiency of the reduced basis technique can be increased if the error tolerance is increased and the accuracy of the reduced system of equations is maintained by backtracking the solution path every time a new (updated) set of basis vectors is generated. However, the backtracking process can only be used when both the external and internal forces are conservative.

4) In cases where rapid changes in the spatial distribution occur in a small region of the shell, a reduced basis substructuring technique (or a partitioning scheme) can be used wherein the basis vectors in the region of rapid change are updated more frequently than the basis vectors in other regions. The reduced basis substructuring technique can also be used in the presence of localized inelasticity.

## Concluding Remarks

A hybrid finite-element Rayleigh-Ritz technique is used to predict the collapse behavior of shells. The computational algorithm presented by the authors in Refs. 6 and 7 is modified to handle the case of loading applied by means of axial end shortening, as would occur in a laboratory compression test. A scalar function is introduced for measuring the degree of nonlinearity of the structure. Also, a quantitative measure for the error of the reduced system of equations is proposed. Some insight is given as to why and when the reduced basis technique works, and the potential of the technique for predicting the collapse behavior of shells is demonstrated by means of a numerical example of elastic collapse of an axially compressed pear-shaped cylinder, wherein over two-orders-of-magnitude reduction in the number of degrees of freedom is achieved.

## References

[1] Besseling, J. F., "Nonlinear Analysis of Structures by the Finite Element Method as a Supplement to a Linear Analysis," *Computer Methods in Applied Mechanics and Engineering*, Vol. 3, March 1974, pp. 173-194.

[2] Besseling, J. F., "Post-Buckling and Nonlinear Analysis by the Finite Element Method as a Supplement to a Linear Analysis," *ZAMM*, Vol. 55, No. 4, April 1975, pp. T3-16.

[3] Nagy, D. A., "Modal Representation of Geometrically Nonlinear Behavior by the Finite Element Method," *Computers and Structures*, Vol. 10, Aug. 1979, pp. 683-688.

[4] Nagy, D. A. and König, M., "Geometrically Nonlinear Finite Element Behavior Using Buckling Mode Superposition," *Computer Methods in Applied Mechanics and Engineering*, Vol. 19, Sept. 1979, pp. 447-484.

[5] Almroth, B. O., Stern, P., and Brogan, F. A., "Automatic Choice of Global Shape Functions in Structural Analysis," *AIAA Journal*, Vol. 16, May 1978, pp. 525-528.

[6] Noor, A. K. and Peters, J. M., "Reduced Basis Technique for Nonlinear Analysis of Structures," *AIAA Journal*, Vol. 18, April 1980, pp. 455-462.

[7] Noor, A. K., Andersen, C. M., and Peters, J. M., "Global-Local Approach for Nonlinear Shell Analysis," *Proceedings of the Seventh ASCE Conference on Electronic Computation*, Washington University, St. Louis, Mo., Aug. 1979, pp. 634-657.

[8] Noor, A. K. and Peters, J. M., "Nonlinear Analysis Via Global-Local Mixed Finite Element Approach," *International Journal for Numerical Methods in Engineering*, Vol. 15, 1980, pp. 1363-1380.

[9] Bergan, P. G., Horrigmoe, G., Kråkeland, B., and Søreide, T. H., "Solution Techniques for Nonlinear Finite Element Problems," *International Journal for Numerical Methods in Engineering*, Vol. 12, No. 11, 1978, pp. 1677-1696.

[10] Hartung, R. F and Ball, R. E., "A Comparison of Several Computer Solutions to Three Structural Shell Analysis Problems," Air Force Flight Dynamics Laboratory, Wright-Patterson AFB, Ohio, AFFDL-TR-73-15, April 1973.

[11] Jones, R. F. and Costello, M. G., "A Solution Procedure for Nonlinear Structural Problems," in *Numerical Solution of Nonlinear Structural Problems*, AMD-Vol. 6, American Society of Mechanical Engineers, 1973, pp. 157-169.